Chapter 4

Re-Os isotope systematics in black shales from the Lesser Himalaya: Their Chronology and role in $^{187}Os/^{186}Os$ evolution of seawater

In this chapter Re-Os isotope systematics in black shales from the Lesser Himalaya is discussed. Re-Os studies in these black shales have been done (i) to explore the possibility of providing chronology for the Krol belt and Tejam Group sediments of the outer and inner sequences of the Lesser Himalaya respectively and to test the various models given for their intercorrelation and (ii) to evaluate the role of these black shales in contributing radiogenic Os to rivers draining them and finally to the oceans. The ages of the sedimentary sequences in the Lesser Himalaya is a controversial topic. There is considerable debate on the ages of these sedimentary rocks either due to the paucity of fossil records or in the interpretation of available few fossils records. The Tal formation of the outer belt (Krol Belt) was initially assigned Permian age (Auden, 1937; Gansser, 1964) but now it is considered to be of Early Cambrian after the discoveries of small shelly and trace fossils of Cambrian origin (Azmi, 1983; Singh and Rai, 1983; Bhatt *et al.*, 1985; Kumar *et al.*, 1987). There are no radiometric ages for these rocks, except the one by Sharma *et al.*, (1992) on the Lower Tal formation. In the absence of ages for the rocks from the inner and outer belts, attempts to inter-correlate them have been hampered.

The $^{187}Os/^{186}Os$ of the oceans has been increasing with time since last ~50 Ma. This increase has been attributed to the intense weathering of the Himalaya (Pegram *et al.*, 1992; Ehrenbrink *et al.*, 1995; Turekian and Pegram 1997) particularly the organic matter rich black shales of the Lesser Himalaya. Black shales are known to contain high Re in them (Ravizza and Turekian, 1989) which over time decays to ^{187}Os making the Os isotope composition in them highly radiogenic. Weathering of such black shales could be an important source of radiogenic Os to the oceans.

As already discussed in Chapter 2 under the Stratigraphy and Lithology of the Area section, black shales occur in both the inner and outer sedimentary belts of the Lesser Himalaya as dispersed units (Gansser, 1964; Valdiya, 1980).

In the outer Lesser Himalaya, black shales are present in the Infra-Krol, Krol and Tal formations extending from Solan in the Himachal Himalaya to Nainital in the Kumaun Himalaya (Fig. 4.1). The black shales associated with the Infra-Krol and Upper Krol formations occur in and around Solan, Mussoorie, Garhwal and Nainital (Fig. 4.1). Black shales are generally more abundant in the Tal formation compared to Infra-Krol

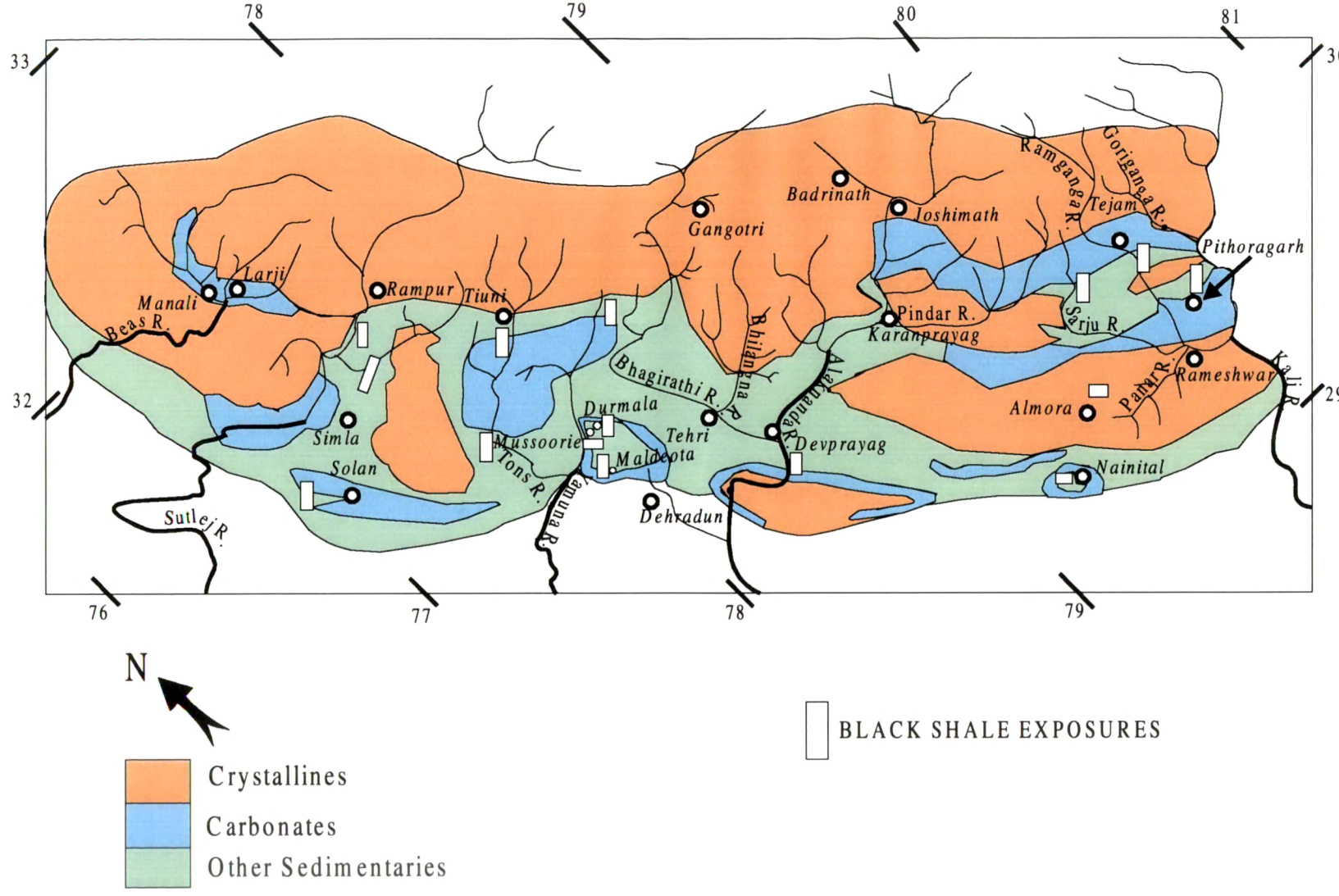

Fig. 4.1: Black Shale occurences in the Lesser Himalaya. Samples for this study collected from some of these locations

and Krol formations. Prominent exposures of these black shales are around Mussoorie, Tehri-Garhwal and Solan

In the inner belt, black shale outcrops are reported (Rupke, 1974) at many locations between the rivers Beas (Himachal Himalaya) and the Kali (Kumaun Himalaya). These are dispersed in the drainage basins of Sutlej (Indus), Tons (Ganga), Sarju and Kali (Ghaghara) and are associated with the calcareous units of the Deoban, Shali and Mandhali formations.

As discussed earlier the stratigraphic correlation between the inner and outer sedimentary belts of the Lesser Himalaya is a topic of debate due to lack of sufficient data on their ages. The debate can be resolved if the chronology of black shales from these inner and outer belts are established. Efforts made in this work, to date the Maldeota and Durmala sections of the outer belt from the Mussoorie region and the inner belt outcrops from Simla is a step in this direction.

4.1 SAMPLES

The samples analysed in this study (Fig. 4.1) are mainly from four regions, selected from various formations of the outer (Nainital, Mussoorie and Almora) and the inner belts (Simla) and were collected during three field campaigns in 1992, 1994 and in 1998. Samples adjacent to Nainital (Fig. 4.1) are from the Upper Krol formation whereas those from the Mussoorie region are from the lower Tal formation. The inner belt samples are from Simla area occurring in the Shali formation. The samples collected fall into two categories, (i) from outcrops to obtain spatial distribution of Os isotope ratios in the Lesser Himalaya. These were collected either from road cuts or from natural exposures and in most cases were sampled a few centimeters below their exposed surfaces to obtain better preserved samples. The samples ranged in colour from grey to black with many of them having laminations and pyrites in them. They were generally compact, however some of them, KU92-49, 50, 51 and UK94-51, 66 were friable. (ii) from the Durmala and Maldeota underground phosphorite mines, near Mussoorie, to explore the use of ^{187}Re-^{187}Os isotope pair to date them. In the Mussoorie hills, a thick succession of Nagthat–Blaini–Infra-Krol–Krol and Tal formations are exposed which

represents the transition from the Proterozoic to the Lower Cambrian (Shanker *et al.*, 1993; see Chapter 2).

4.2 Org. C, N, Re, Os CONCENTRATIONS AND $^{187}Os/^{186}Os$

The concentrations of organic carbon, nitrogen, Re and Os and $^{187}Os/^{186}Os$ in the black shale samples were measured by procedures outlined in Chapter 2. The results for the outcrop samples are given in Table 4.1, and those for the Maldeota and Durmala underground mine samples in Table 4.2. The Re and Os concentrations and $^{187}Os/^{186}Os$ isotopic ratios given in Tables 4.1 and 4.2 are uncorrected for blank as they were considerably less than the sample values (Chapter 2).

The organic carbon and nitrogen content of the samples are in the range of 0.2 to 7.3 % and 0.02 to 0.27 % respectively (Tables 4.1, 4.2). The mean organic C in the mine and outcrop samples overlap within errors, however, the outcrop samples are characterised by lower organic C with many of them having <1%. In this work all these samples are considered as black shales, though there is some debate as to whether samples with <1% organic C can be included in this category (Arthur and Segeman, 1994; Meyer and Robb, 1996; Pasava *et al.*, 1996). The Re and Os concentrations in the samples show a wide range, 0.2-264 ng g^{-1} and 0.02 to 13.5 ng g^{-1}respectively (Tables 4.1, 4.2; Fig. 4.2). The outcrop samples generally have <20 ng Re g^{-1} whereas those from the mines exhibit a wider range, with a significant number of samples having Re in excess of 50 ng g^{-1}. The $^{187}Os/^{186}Os$ also shows wide range 8.465 to 96.099, however, bulk of the samples have ratio between 10-30 (Fig. 4.2).

The covariation between Re and organic C and ^{192}Os and organic C are plotted in Fig. 4.3. The correlation coefficient between Re and organic carbon is 0.45 which increases to 0.59 if only samples with <20 ng Re g^{-1} are considered. Similarly, the correlation coefficient for the ^{192}Os vs organic carbon is 0.24 which increases to 0.65 if only the samples having <1 ng g^{-1} ^{192}Os are used for the regression. Plots of Re and ^{192}Os against nitrogen using it as the index of organic matter (Fig. 4.3) also give correlation coefficient which are similar to those derived based on the organic carbon data. The covariations of Re and ^{192}Os with organic carbon and nitrogen indicate their overall affinity with organic matter as observed by earlier workers (Ravizza and Turekian, 1989, 1992; Ravizza *et al.*, 1991; Colodner *et al.*, 1993).

Table 4.1: Re, Os abundances and Os isotopic composition of black shale outcrops from the Lesser Himalaya

Region & Sample #	Org. C (% wt.)	N (% wt.)	Os (ng g^{-1})	Re (ng g^{-1})	$^{187}Re/^{186}Os^{\$}$	$^{187}Os/^{186}Os^{\$}$
			Outer Belt Samples			
Dehradun-Mussoorie						
KU92-53*	1.62	0.02	0.83	16.9	946 ± 100	12.376 ± 0.030
KU92-57	5.11	0.22	0.65	5.48	425 ± 13	18.608 ± 0.176
UK94-51	2.98	0.12	4.13	-	-	10.134 ± 0.026
UK94-66	4.00	0.26	0.65	-	-	22.447 ± 0.178
UK94-52	0.76	0.04	0.05	0.52	439 ± 13	12.340 ± 0.396
UK94-53	1.05	0.05	0.13	3.56	1418 ± 69	20.901 ± 0.104
UK94-54	0.71	0.04	-	0.51	-	-
UK94-55	0.54	0.04	0.04	0.35	415 ± 40	13.908 ± 0.120
UK94-56	0.65	0.04	0.08	1.55	961 ± 69	17.353 ± 0.800
UK94-58	0.21	0.02	0.02	0.22	524 ± 71	14.263 ± 0.400
Nainital						
KU92-51*	0.82	0.06	-	6.41	-	-
KU92-50*	0.91	0.05	-	3.54	-	-
KU92-49	0.91	0.06	0.08	5.18	3713 ± 290	29.820 ± 0.458
Almora						
KU92-2	5.38	0.06	0.04	-	-	8.465 ± 0.452
KU92-6	5.85	0.03	0.51	-	-	26.679 ± 0.097
			Inner Belt samples			
Simla						
HP94-22*	3.95	0.27	0.18	13.1	7216 ± 1113	96.099 ± 2.859
HP94-24	1.01	0.08	0.05	1.16	1260 ± 133	24.920 ± 0.450
HP94-25	2.15	0.16	0.10	-	-	74.336 ± 3.366
HP94-26	0.67	0.12	0.05	0.87	867 ± 53	17.757 ± 0.212

$ errors are ± 2σ on the mean for $^{187}Os/^{186}Os$ and ± 2 s.d. for $^{187}Re/^{186}Os$.

* Re measurement by wet oxidation; others by ashing at 450°C followed by acid digestion (see Chapter 2).

Table 4.2: Re, Os and $^{187}Os/^{186}Os$ in black shales from the Maldeota and Durmala mines

Region & Sample #	Org. C (% wt.)	N (% wt.)	Os (ng g^{-1})	Re^{+} (ng g^{-1})	$^{187}Re/^{186}Os^{\$}$	$^{187}Os/^{186}Os^{\$}$
Maldeota						
UK98-1	3.88	0.17	0.60	8.64	710 ± 23	15.373 ± 0.093
UK98-2	4.73	0.20	1.57	68.6	2564 ± 72	30.490 ± 0.164
UK98-3	2.58	0.14	2.63	153	4340 ± 205	57.548 ± 0.126
UK98-4	1.01	0.16	0.17	3.16	945 ± 87	15.923 ± 0.439
UK98-8	4.87	0.18	0.42	5.37	628 ± 29	16.638 ± 0.084
UK98-9	5.04	0.19	0.40	5.10	612 ± 71	14.790 ± 0.452
UK98-11	4.69	0.17	0.57	13.4	1225 ± 89	21.384 ± 0.169
KU92-56*	3.97	0.17	13.5	264	975 ± 32	18.002 ± 0.134
KU92-58*	4.57	0.20	0.79	18.8	1217 ± 9	19.864 ± 0.139
Durmala						
UK98-17	7.28	0.23	2.84	115	2373 ± 106	31.853 ± 0.179
UK98-18	7.25	0.23	3.14	122	2249 ± 102	30.702 ± 0.232
UK98-19	3.06	0.14	0.34	7.22	1078 ± 42	19.271 ± 0.180
UK98-28	2.85	0.14	0.31	3.05	470 ± 15	14.450 ± 0.155
UK98-31	2.75	0.14	0.41	6.48	791 ± 24	18.141 ± 0.227

$ errors are ± 2σ on the mean for $^{187}Os/^{186}Os$ and ± 2 s.d. for $^{187}Re/^{186}Os$.

\+ all Re measurements by ashing at 450°C followed by acid digestion except where indicated.

* Re measurements by wet oxidation. These two samples were not collected from the mine, but were picked up from the mined material outside.

In general, Re concentration, organic carbon and Re/Os (mean 25; range 8-73) in black shales from the Lesser Himalaya are lower than those reported for the Bakken, New Albany, Chattanooga (Ravizza and Turekian, 1989; Ravizza, 1991) and Canadian (Horan *et al.* 1994) black shales. The low organic carbon content of black shales from the Lesser Himalaya may be contributing to their low Re and Re/Os. Other possible

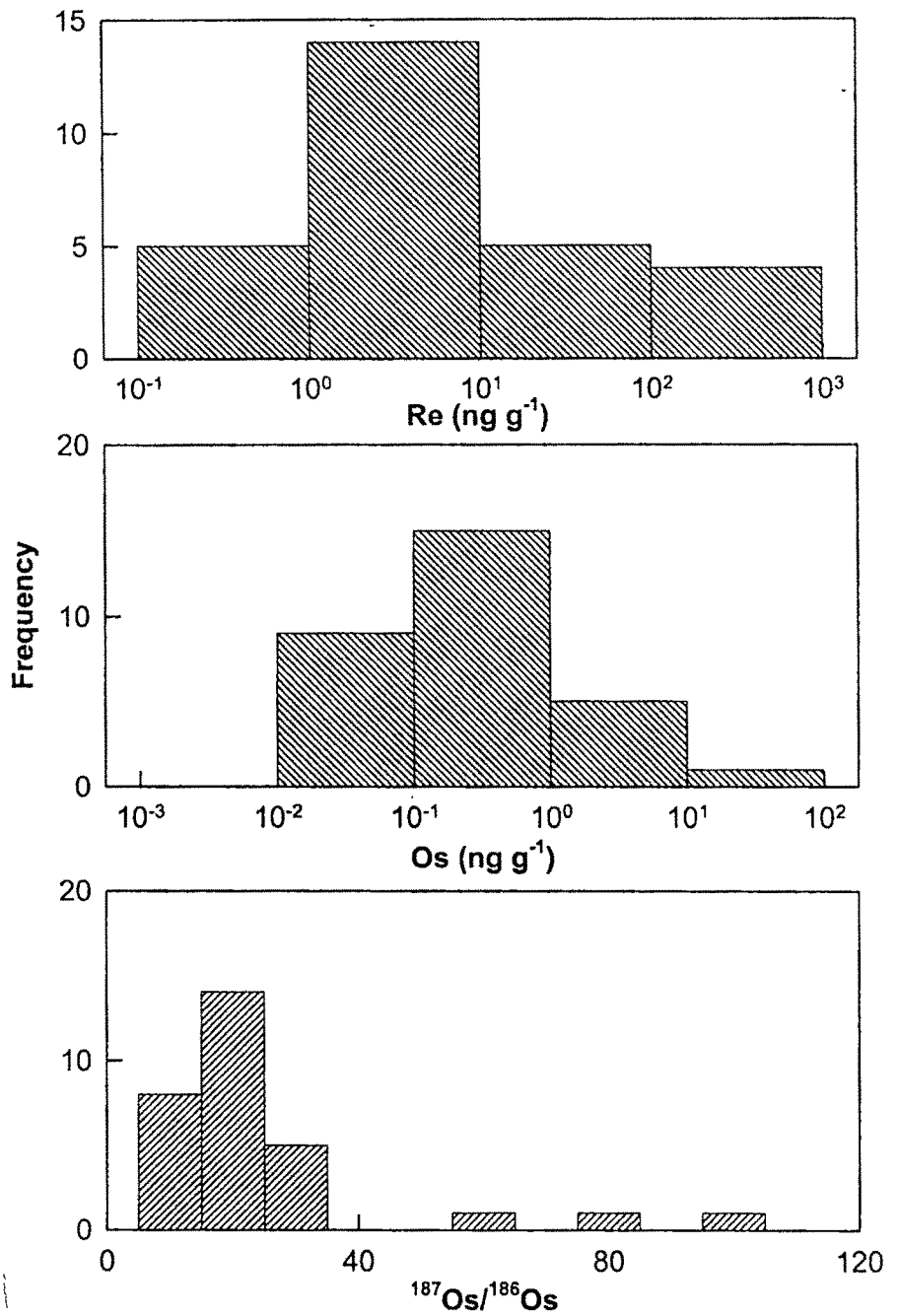

Fig. 4.2: Histograms of Re, Os concentrations and $^{187}Os/^{186}Os$ in the Lesser Himalayan black shales.

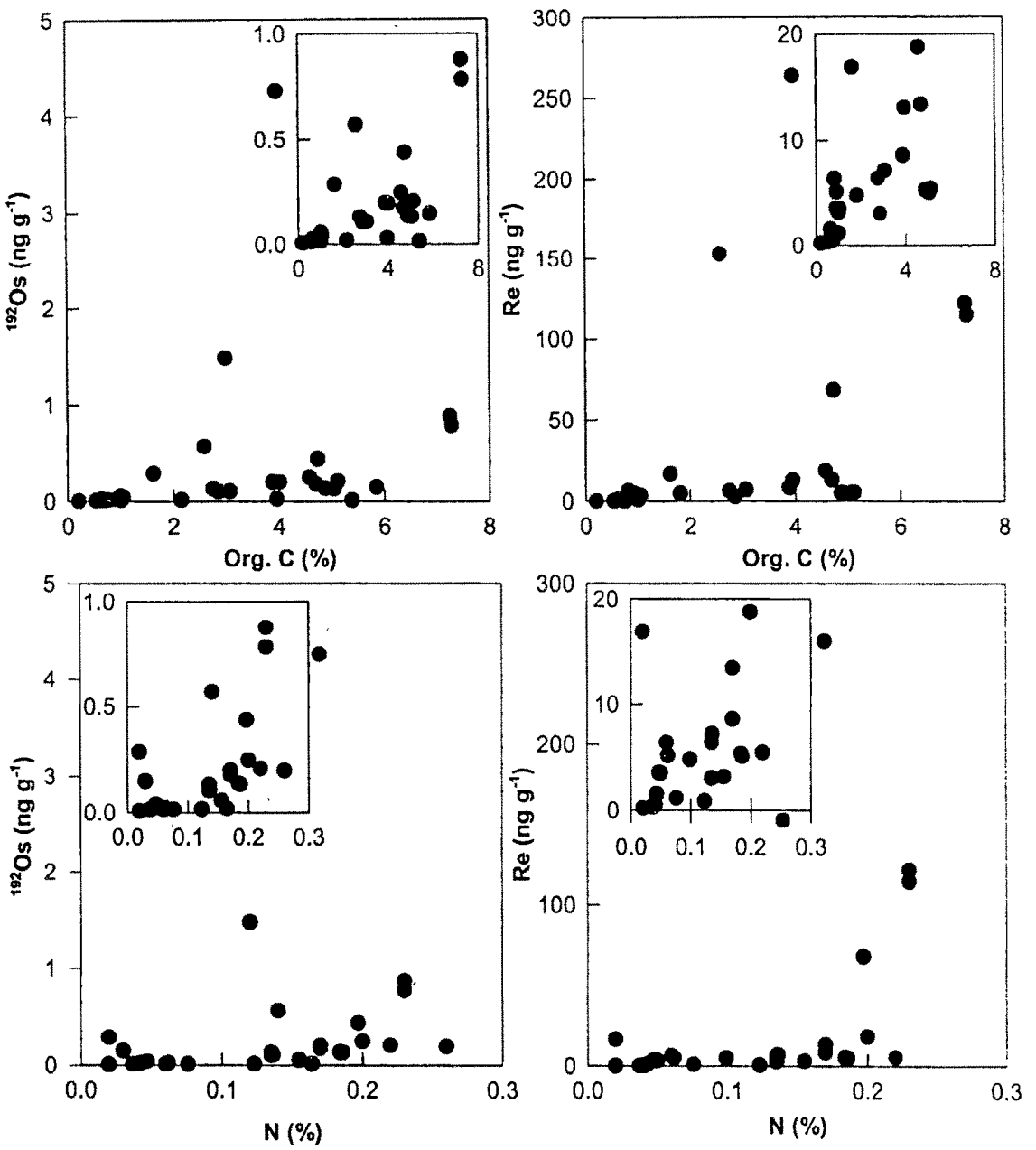

Fig 4.3: Covariation diagrams of ^{192}Os and Re with organic carbon and Nitrogen. Both ^{192}Os and Re show positive correlation with organic carbon and nitrogen.

Table 4.3: Major and minor element data for black shales

Sample	Al	Fe	Mg	Ca	Na	K	Mn	P	V	Cu	Re
KU92-49	12.86	2.93	1.54	0.09	0.29	6.28	38	282	167	7	5.18
KU92-50	11.57	2.59	1.26	0.02	0.11	5.21	46	193	121	14	3.54
KU92-51	10.62	3.86	2.79	1.37	0.22	5.51	598	321	72	44	6.41
KU92-53	0.47	0.30	0.45	0.92	0.15	0.30	100	493	136	23	16.9
KU92-56	6.47	2.49	2.08	4.68	0.21	3.14	213	10678	2643	101	264
KU92-57	7.77	4.84	1.18	1.46	1.38	3.37	207	943	118	60	5.48
KU92-58	7.82	4.52	1.17	0.12	1.33	2.13	192	658	59	66	18.8

All concentrations in % except for Mn, P, V and Cu which are in ppm and Re in ppb

explanations for this observation could be (i) water from which the black shales from the Lesser Himalaya were formed had lower Re and Re/Os (ii) loss of Re by weathering and mobilization. This seems an unlikely proposition considering the presence of fresh shining pyrites in many of them and considering that samples from the underground mines yield good isochrons with ages that are stratigraphically consistent (discussed below).

Major element composition for some of the black shales (Table 4.3) show that they are similar to shales except for the sample KU92-53, which is a chert, collected from the chert-phosphorite layer of the Tal formation. The covariations between Re vs P, V and Cu show positive correlations. The correlation coefficients between Re vs P, V and Cu are 0.997, 0.996 and 0.754 respectively which indicate the association of all these elements with organic matter.

4.3. LESSER HIMALAYAN BLACK SHALE CHRONOLOGY

The chronology of black shales from the Maldeota and Durmala mines from the outer belt of the Tal formation and Shali formation of the inner belt are discussed in this section. The period of deposition of the various sedimentary sequences in the Lesser Himalaya, based on fossil records and the intercorrelation between them was summarised in Chapter 2.

Based on the lithological settings and fossil records, many workers have correlated the Inner and Outer belts of the Lesser Himalaya to understand their origin and

tectonic settings. These were discussed in detail in Chapter 2 and the two models of correlation are briefly presented below. West (1939), Frank and Fuchs (1970) and Valdiya (1995) have correlated Deoban (Shali) formation of the inner belt to the Krol formation of the outer belt and Mandhali of the inner to the Tal of the outer belt based on the similarities in their lithologies and the formations underlying them. Mehr (1977) and Stocklin (1980) on the other hand based on structure and Shanker *et al.* (1993) based on the fossil records have suggested that the inner belt rocks are older than those of outer belts. Sharma *et al.*, (1992) have reported an age of 626±13 Ma for black shales from the chert-phosphorite unit of the lower Tal formation using Rb-Sr systematics. This unit is just above Krol-Tal boundary and about 10 m below the black shale band dated in this study using Re-Os.

Dating sedimentary rocks is difficult as the setting of radiometric clocks in them is not straightforward. The isotopic composition of sedimentary rocks often contain in them signatures of the rocks from which they are formed and thus serve more as tracers to tag the provinance from where they were derived, rather than as geochronometers. In addition, possible open system behaviour of both parent and daughter nuclides during weathering and burial diagenesis makes the application of the commonly used isotope pairs to date them difficult. In this context, Rb-Sr pair has met some success (Faure, 1986) when < 2 μm clays are separated from sedimentary rocks and analysed for their Rb-Sr. Meaningful ages has been obtained using this technique for the sedimentary rocks (Gorokhov *et al.*, 1981).

More recently, Ravizza and Turekian (1989) demonstrated the potential of ^{187}Re-^{187}Os isotope pair as a chronometer for black shales. Depositional enrichment of Re and Os in organic rich sediments sets the Re-Os system apart from other long-lived decay schemes and makes it a potentially viable tool for black shale geochronometry. Re and Os both are siderophilic and chalcophilic and are scavenged from seawater at the time of black shale deposition. The scavenged component of Re and Os generally overwhelms their detrital components.

^{187}Re decays to ^{187}Os by beta decay with a decay constant of 1.64×10^{-11} y^{-1} (Lindner *et al.*, 1989). The equation which describes the changes in the $^{187}Os/^{186}Os$ ratio with time is given as

$$\left(\frac{^{187}Os}{^{186}Os}\right)_t = \left(\frac{^{187}Os}{^{186}Os}\right)_o + \left(\frac{^{187}Re}{^{186}Os}\right)_t \times \left(e^{\lambda t} - 1\right)$$

where,

$\left(\frac{^{187}Os}{^{186}Os}\right)_t$ and $\left(\frac{^{187}Re}{^{186}Os}\right)_t$ are the present day atomic ratios measured in the sample.

$\left(\frac{^{187}Os}{^{186}Os}\right)_o$ is the atom ratio of the system at the time of closure.

λ is the decay constant of ^{187}Re.

In this context the time of closure designate the point in time after which neither Re nor Os are lost from or added to the system. To get a meaningful age, which corresponds to the time of deposition, following assumptions have to be valid:

(i) initial $^{187}Os/^{186}Os$ is homogeneous i.e. at the time of deposition $^{187}Os/^{186}Os$ was uniform in the basin and

(ii) the Re-Os system has remained closed since the time of closure, i.e. there is no gain or loss of Re-Os from the black shales since they were formed.

For a set of closed, coeval whole-rock samples with variable Re/Os ratios which are fulfilling above conditions, a plot of $(^{187}Os/^{186}Os)_t$ vs $(^{187}Re/^{186}Os)_t$ will yield a colinear array of points with slope of $(e^{\lambda t}-1)$. The array of points is known as an isochron. The amount of time which has been elapsed since the deposition of the rock can be calculated from the slope of the isochron and λ, the decay constant.

In this work, ^{187}Re-^{187}Os isotope pair has been used to date the black shale samples from both the inner and the outer Lesser Himalaya.

(i) Outer belt black shales

In the outer Lesser Himalaya samples were collected for Re-Os chronology from two underground mines which are are at the two limbs of Mussoorie syncline, near Mussoorie. Rock phosphate is mined from these mines. Maldeota, one of these two mines is situated on the eastern limb whereas Durmala is on the western limb of the syncline. The lithological section of these mines has been already shown in Chapter 2. Above the chert-phosphorite unit of the Lower Tal formation is the black shales of argillaceous unit. Samples for Re-Os chronology were collected from this argillaceous layer (Fig. 4.4). In

Maldeota, seven samples were collected from the same horizon (lateral distance of ~1km) at three different elevations in the direction of the bed strike. Two samples, KU92-56 and KU92-58, from the same horizon but are samples from an earlier sampling trip picked from the pile kept outside the mine. In Durmala, five samples were collected from the same horizon at two different locations separated by a distance of ~3-4 km. In

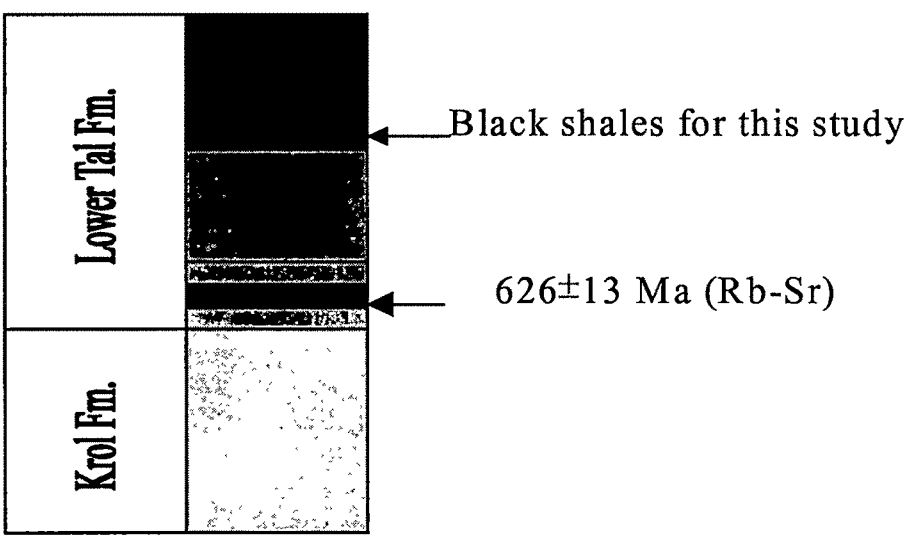

Fig. 4.4 Black shale samples collected in this study for chronology. The samples are ~10 m above the Krol-Tal boundary. Also shown is the age of black shale in the chert-phosphorite layer by Rb-Sr dating (Sharma *et al.*, 1992)

hand specimens, these mine samples are black and indistinguishable from each other. They were compact with thin laminations. Thin horizons rich in pyrite were common and in some cases small pyrite concretions were also encountered.

A total of 14 samples were analysed from the Maldeota and the Durmala mines for their Re, Os concentrations, $^{187}Os/^{186}Os$ and organic carbon (Table 4.2; Singh *et al.*, 1999). The Organic carbon contents of the samples are in the range of 1.01% to 7.28%. The Re and Os concentrations in the samples show a wide range and vary from 3.05 to 264 and 0.17 to 13.5 ng g^{-1} respectively. The age of the black shale formations from the Maldeota and Durmala mines can be determined from their $^{187}Os/^{186}Os$ vs $^{187}Re/^{186}Os$ plot if they satisfy the assumptions discussed earlier. With the data in Table 4.2 best-fit line is drawn following Williamson (1968) to derive their ages and initial ratio with associated errors (Singh *et al.*, 1999). This yield ages of 554 ± 16 Ma and 552 ± 22

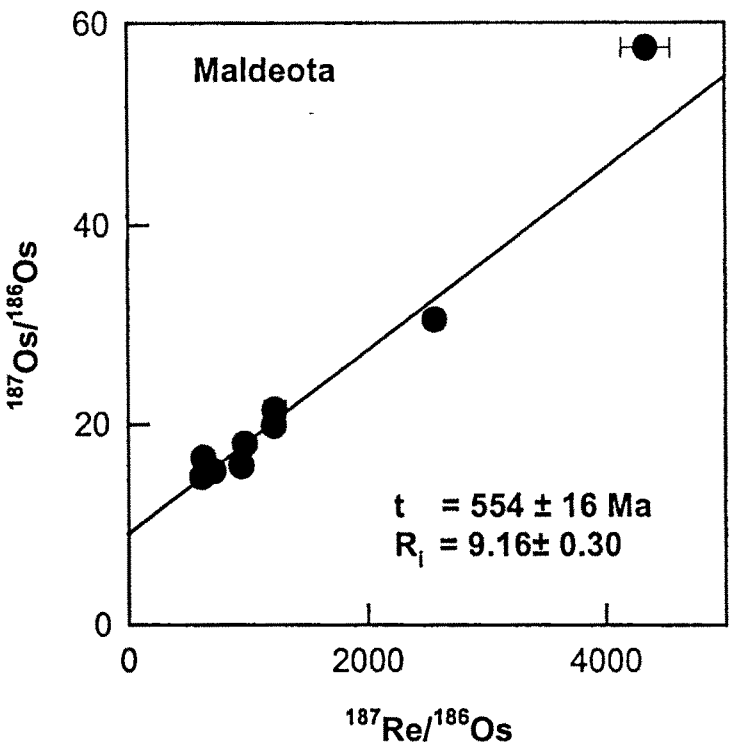

Fig. 4.5: Isochron plot for black shales from Maldeota mine. The isochron age (t) obtained and initial $^{187}Os/^{188}Os$ (R_i) is given (Singh *et al.*, 1999).

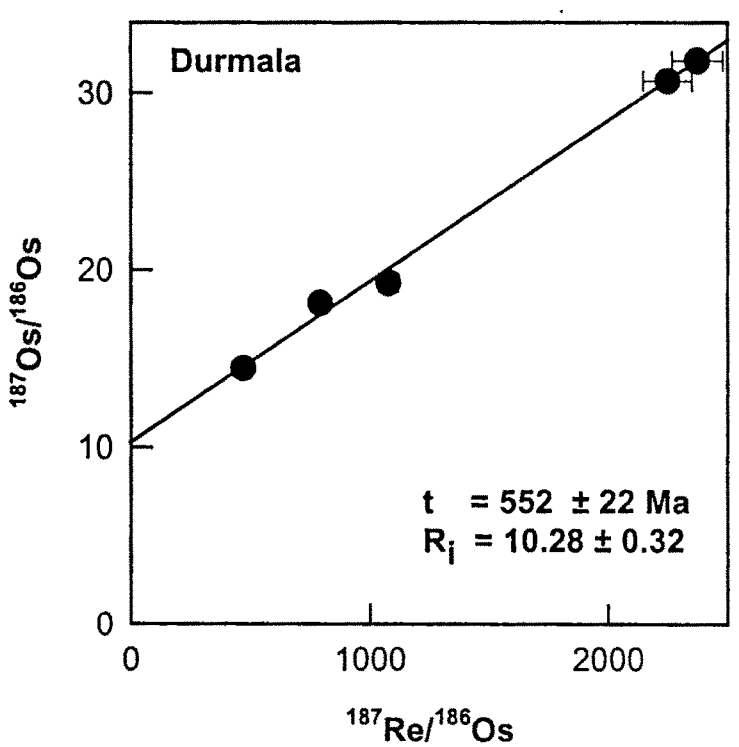

Fig. 4 6: Isochron plot for black shales from the Durmala mine. The age is 552 ± 22 Ma with an initial ratio of 10.28 ± 0.32 (Singh *et al.*, 1999).

Ma (± 2σ) for the Maldeota (Fig. 4.5) and the Durmala (Fig. 4.6) black shales (calculated using ^{187}Re decay constant of 1.64×10^{-11} y^{-1}, Lindner *et al.*, 1989) with initial $^{187}Os/^{186}Os$ ratios of 9.16 ± 0.30 and 10.28 ± 0.32 (±2σ) respectively.

Since black shales from both the mines were collected from the same stratigraphic horizon and from same lithological settings as shown in Fig. 4.4, they can be plotted

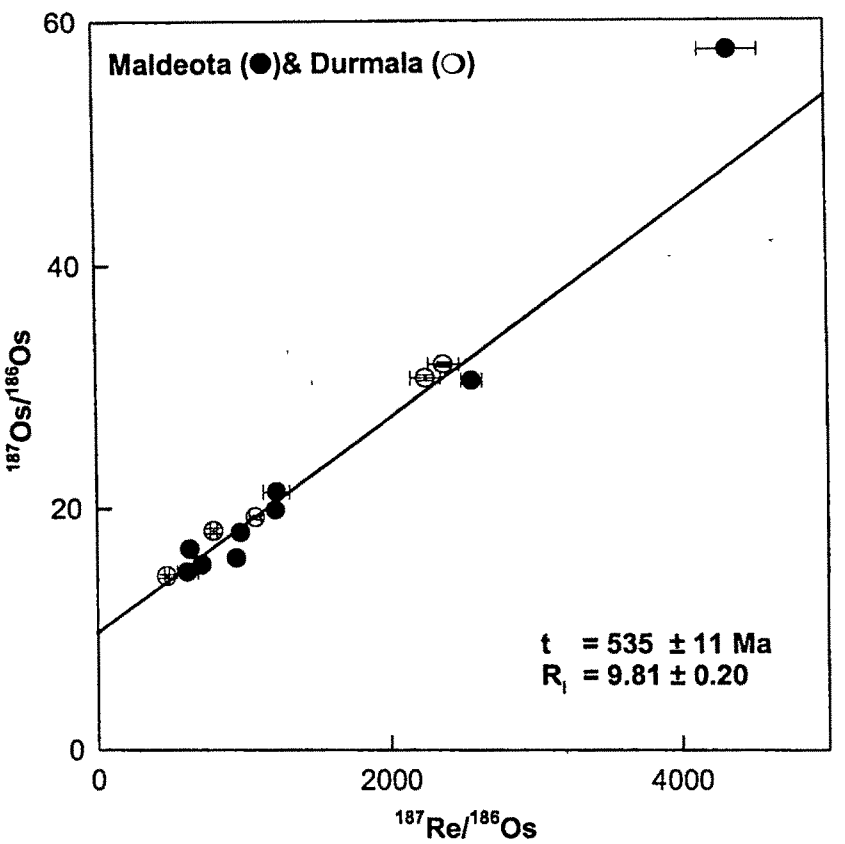

Fig. 4.7: ^{187}Re-^{187}Os isochron plot for data from both the mines, the Maldeota and Durmala. The pooled data yield an age of 535 ± 11 Ma same within errors of those obtained for the individual mines (Singh *et al.*, 1999).

together. Pooling the data together (Fig. 4.7) gives an age of 535 ± 11 Ma with an initial ratio of 9.81 ± 0.20. All the isochron ages obtained for samples from both the underground mines and their pooled data are same within experimental uncertainties. In order to assess the influence of "mixing" in generating the isochron plot (Figs. 4.5-4.7) $^{187}Os/^{186}Os$ were plotted against $1/^{192}Os$. The plots do not exhibit any systematic trend, ruling out the possibility of mixing as a cause for the observed isochron.

The Maldeota and Durmala mine samples are from the Lower Tal formation, ~15 m above the Upper Krol/Lower Tal (Pc-C) boundary (Fig. 4.4). The ^{187}Re-^{187}Os isochron ages obtained for black shales in this study; 535 ± 11 Ma is consistent with the Early Cambrian age assigned to the lower Tal formation based on the presence of trace fossils and microfauna in them (Azami, 1983; Singh and Rai, 1983). The Re-Os ages, however, are about 70 Ma younger than the Rb-Sr age of black shales from the chert-black shale layer collected from a location near the Maldeota mine (Sharma *et al.*, 1992). Their samples, occurring ~10 m below the black shale band dated in this study (Fig. 4.4), yield an age of 626 ± 13 Ma.

Aharon *et al.* (1987) Shanker *et al.*, (1993) have correlated the Lower Tal formation with the Tomotian stage of the stratotype section of Siberia based on fossil assemblages. U-Pb dating of zircons separated from volcanic braccia contained in the basal part of the Tommotian yield a maximum age of 534.6 ± 0.4 Ma (Bowring *et al.*, 1993). In another section in the Olenek region Bowring *et al.* (1993) have reported an U-Pb age of 543.6 ± 0.24 Ma for zircons from volcanic braccia occuring within the Nemakit-Daldynian Stage. Based on this age they have estimated an age of 544 Ma for Pc-C boundary. The chert member (with phosphorite) of the Lower Tal formation is also correlated with the Meishucunian Zone of South China (Fig. 4.8). Rb-Sr ages of black shales deposited just above the Pc-C boundary in the Meishucunian section, Yunnan province is 579.7 ± 8.2 Ma (Xue 1984). Zhang *et al.* (1984) have reported Rb-Sr ages ranging between 569 to 602 Ma for samples collected just above the Pc-C boundary from various Chinese sections. Recent data from U-Pb isochrons from ash bands near marker B of Mishucunian section indicate a much younger age of 525 ± 7 Ma (Compston *et al.*, 1992). It is seen from these comparisons that the Rb-Sr ages obtained for the Pc-C boundary are generally a few tens of million years older (569-626) than those based on U-Pb dating of zircons (520-545 Ma) separated from volcanic ash contained in the Early Cambrian sedimentary rocks in Canada, Morocco, China, Siberia and South Australia (Bowring *et al.* 1993; Brasier *et al.* 1994).

The Re-Os age of black shales analysed in this study, 535 ± 11 Ma, deposited ~15 m above Pc-C boundary is consistent with these U-Pb ages of the Tommotian and

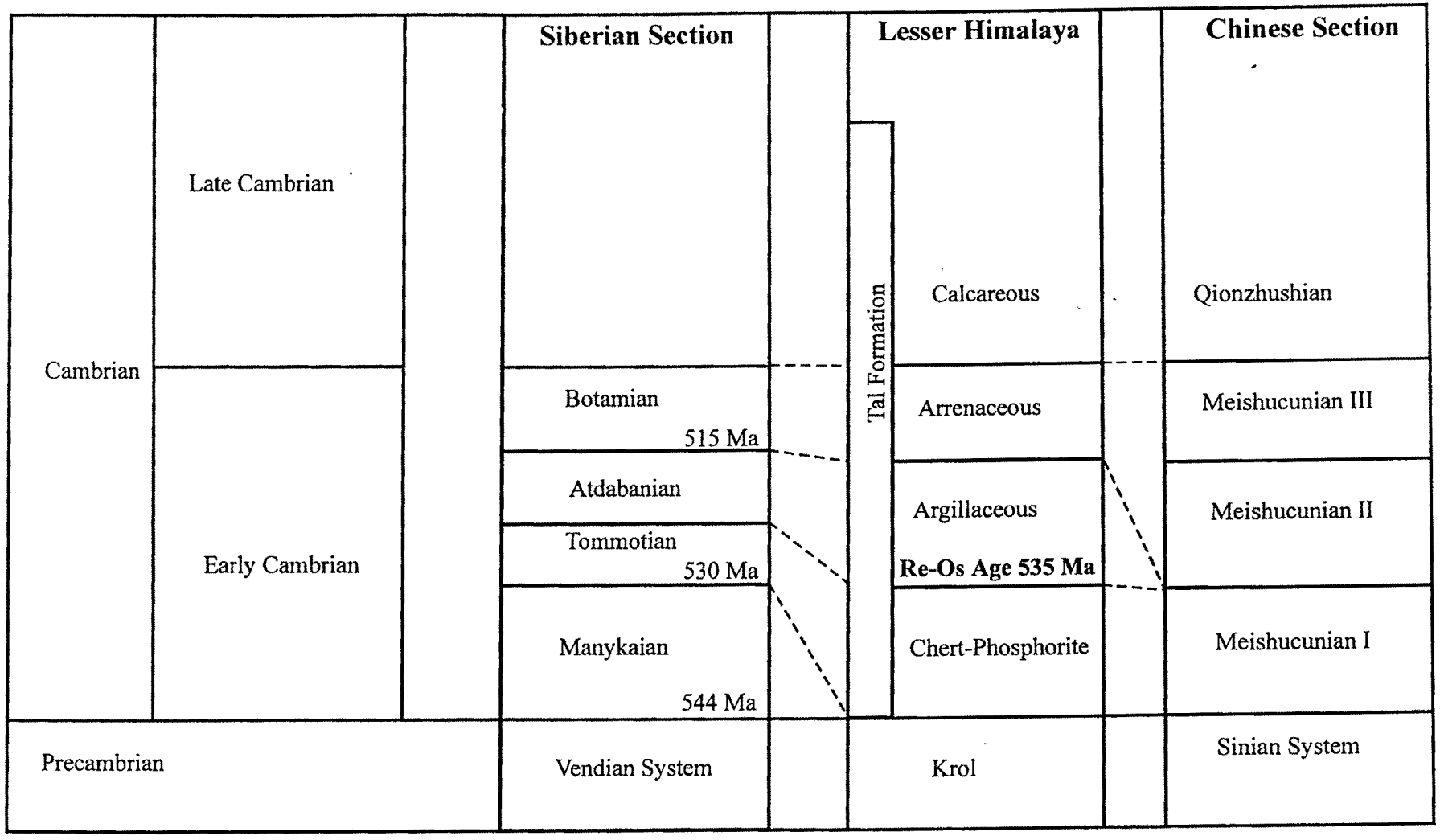

Fig 4.8: Correlation of different units of Tal formation of the Lesser Himalaya with Siberian and Chinese stratotype sections based on the fossil records. Ages for the Manykaian-Tommotian and Atdabanian-Botamian boundaries are based on U-Pb dating of zircon collected from volcanic ash near the boundaries (Bowring *et al*., 1993), whereas the age of Pc-C boundary (~544 Ma) is estimated based on various U-Pb ages of zircons (Brasier *et al*., 1994).

Mishucunian sections. The Re-Os chronology along with the available fossil records confirm the identity of Krol-Tal boundary as the Pc-C boundary.

(ii) Inner Belt Samples

Three black shale outcrop samples were analysed from the inner belt of the Lesser Himalaya for their Re, Os concentrations and $^{187}Os/^{186}Os$ (Table 4.1). These samples were collected from road cuts. The data are plotted as an isochron in Fig. 4.9. The isochron age obtained from the slope of the line (Fig. 4.9) is 839 ± 138 (± 2σ) with an initial $^{187}Os/^{186}Os$ ratio of 5.98 ± 2.28.

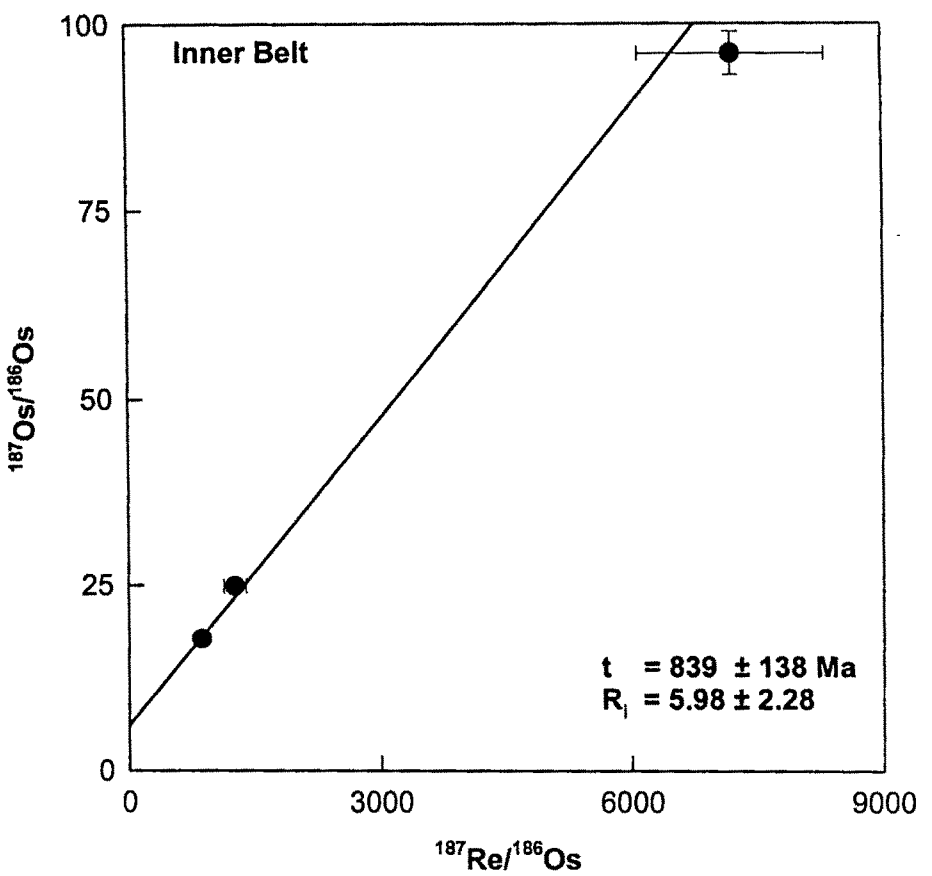

Fig. 4.9: ^{187}Re-^{187}Os isochron diagram for the inner belt black shales. The results yield an age of 839 ± 138 Ma, a few hundred million of years older than the outer belt samples. (Singh *et al.*, 1999).

These results seem to indicate that the inner belt samples are older than the outer belt (Maldeota and Durmala) samples; though the uncertainties associated with the age and the initial ratio of the former are large to make a critical assessment. More inner belt

black shale samples have to be analysed to check on the preliminary results obtained in this study. If these preliminary results, however, are confirmed through more analysis then it would support the model proposed by Mehr (1977), Stocklin (1980) and Shanker *et al.*, (1993) that the inner belt samples were deposited much earlier than the outer belt and making the simple correlation based only on lithology questionable.

It is, however, noteworthy that even if the inner belt sequences (Deoban, Mandhali) are older than those of the outer belt (Krol-Tal) it is difficult from the available information to distinguish whether the outer belt sediments are allochthonus or autocthonus. Three scenerios are possible for their present occurrence in the inner and outer belts. (i) they are allocthonus i.e., they were deposited in the same basin above the Mandhali in the inner belt, but displaced southward along with the crystalline Klippe to the present position due to tectonic activities or (ii) they were deposited in the present location at the beginning or (iii) both the inner and outer belt were depositing in the same basin, but after the deposition of Mandhali, the basin got uplifted near the inner belt. Therefore, the sea regressed southward and deposition continued in the outer belt but stopped in inner belt (Sharma, 1998). A great deal more systematic geological surveying and regional large-scale mapping is needed to choose between these scenarios.

(iii) Os isotopic ratio of Early Cambrian seawater

It is established that the $^{187}Os/^{186}Os$ of the seawater has been increasing with time through the Cenozoic (Pegram *et al.*, 1992, Ravizza, 1993, Ehrenbrink *et al.*, 1995; Turekian and Pegram, 1997; Reusch *et al.*, 1998). Information on longer-term variations in $^{187}Os/^{186}Os$ of seawater, if any, has to be derived from samples deposited during various times in the past and which contain records of seawater Os in them. Black shales may satisfy these requirements as the Os concentration in them is generally dominated by seawater component and samples of different ages can be obtained. The initial $^{187}Os/^{186}Os$ ratios obtained from the isochron plots of black shale Re-Os data is likely to be that of the seawater $^{187}Os/^{186}Os$ of that time as most of the Os in them is derived from seawater. It is seen that the $^{187}Os/^{186}Os$ of modern organic rich sediments is almost equal to the present day seawater value (Ravizza and Turekian, 1992). Thus by dating black shales of the various age groups, it should in principle be possible to obtain the $^{187}Os/^{186}Os$ at the time of their deposition, which in turn can be used to reconstruct Os

evolution curve of ocean through the Phanerozoic and part of Proterozoic times. Uncertainties in the approach include (i) the possibility of inhomogeneous $^{187}Os/^{186}Os$ ratio in the basin due to the local scavenging of Os or incomplete mixing of seawater, (ii) open system behavior of Re-Os system during later diagenesis and weathering resulting in the migration of Re and/or Os (Ravizza and Turekian, 1989) and (iii) contribution from detrital material, which can cause the $^{187}Os/^{186}Os$ of black shales to be different from that of seawater from which they deposit.

The black shale samples from the Maldeota and Durmala mines are of Early Cambrian age. The $^{187}Os/^{186}Os$ initial ratio obtained for these samples should be that of sea-water of that time, if Os in these black shales is derived almost entirely from it and if the seawater reservoir was well mixed. As the residence time of Os is much more than the mixing time of the ocean (Sharma *et al.*, 1997), it is very likely that the later condition is met. The average Os concentration in the black shale samples from the two mines is ~2 ng g^{-1}, ~ 50 times higher than the average crustal value ~0.04 ng g^{-1} (Esser, 1991; Shirey and Walker, 1998). Even the lowest Os measured in these samples, 0.17 ng g^{-1} (Table 4.2) is a factor of ~4 higher than its crustal abundance. It is, therefore, very likely that the initial $^{187}Os/^{186}Os$ ratio in many of these black shales is dominated by seawater component, however, in the low Os samples the influence of crustal component in determining the initial $^{187}Os/^{186}Os$ could be important.

Ravizza (1991) reported initial ratios of 13.1 ± 1.6 and 6.4 ± 3.0 in black shales deposited 354 ± 14 and 358 ± 47 Ma ago. Sluggish ocean circulation and enhanced Os burial have been held responsible for such a large heterogeneity in the initial ratios of samples deposited at about the same time. Such large differences in the initial $^{187}Os/^{186}Os$ ratio in samples deposited at about the same time raises doubt about their use to obtain $^{187}Os/^{186}Os$ of seawater. Our results on the Maldeota and Durmala black shales deposited at ~535 Ma ago yield initial ratios 9.16 ± 0.3 and 10.3 ± 0.3 (Figs. 4.9 and 4.10) which are outside ± 2σ errors.

The differences observed in the two initial Os isotopic ratios at 535 Ma may be due to the differences in the relative proportions of detrital and marine Os incorporated in the black shales during their formation. These results suggest the need to evolve suitable methods to correct for the detrital contribution which would enable the retrieval of the Os

isotope composition of seawater at the time of their deposition from the black shale data. If the endmember composition of the detrital component and its contribution to the black shales can be obtained based on suitable elemental/isotopic proxies, it may be possible to derive seawater Os isotopic composition from the initial $^{187}Os/^{186}Os$ of black shale based on two component mixing model. The problem may be compounded in case of sediments with low accumulation rate where extraterrestrial contribution of Os may become significant.

The value of 9.81 ± 0.20 obtained in this study from the pooled data would seem to indicate that the seawater $^{187}Os/^{186}Os$ was higher 535 Ma ago compared to the present day value of 8.7 (Sharma *et al.*, 1997), however, the interpretation of the data needs better constraints on the crustal contribition.

4.3. Os ISOTOPES IN THE HIMALAYAN BLACK SHALES AND $^{187}OS/^{186}Os$ EVOLUTION OF SEAWATER

The $^{187}Os/^{186}Os$ of seawater is increasing with time since the Cenozoic (Pegram *et al.*, 1992; Ravizza, 1993; Ehrenbrink *et al.*, 1995; Turekian and Pegram, 1997). The Os isotopic composition of the seawater is determined by the mixing proportions of Os derived from three sources: (i) the mantle (hydrothermal supply and submarine basalt weathering) (ii) extraterrestrial and (iii) the currently eroding continental crust (Fig. 4.10). The first two sources have $^{187}Os/^{186}Os$ of ~1 whereas the crustal source is far more radiogenic with $^{187}Os/^{186}Os$ of 10-15 (Shirey and Walker, 1998). The available results on Os isotope evolution (op. cit.) show that at ~65 Ma it was as low as ~2 resulting from extraterrestrial impact which drastically decreased the sea water $^{187}Os/^{186}Os$. This steadily increased and reached a value of ~6 at about 30 Ma (Fig. 4.11). During the time interval of 28-16 Ma the seawater $^{187}Os/^{186}Os$ was nearly constant. From 16 Ma to 1.5 Ma it increased from 6.2 to ~7.7 and then rapidly to the present day value of 8.7 (Fig. 4.11). The general increase of $^{187}Os/^{186}Os$ in the ocean is similar to that observed for $^{87}Sr/^{86}Sr$ (Pegram *et al.*, 1992). The steady increase in the Sr isotope composition has been attributed to weathering and transport of radiogenic Sr from the Himalaya (Richter *et al.*, 1992). Various evidences, such as high $^{87}Sr/^{86}Sr$ in rivers draining the Himalaya, particularly in the Ganga-Brahmaputra, their moderate Sr concentration, the timing of $^{87}Sr/^{86}Sr$ increase, all seem

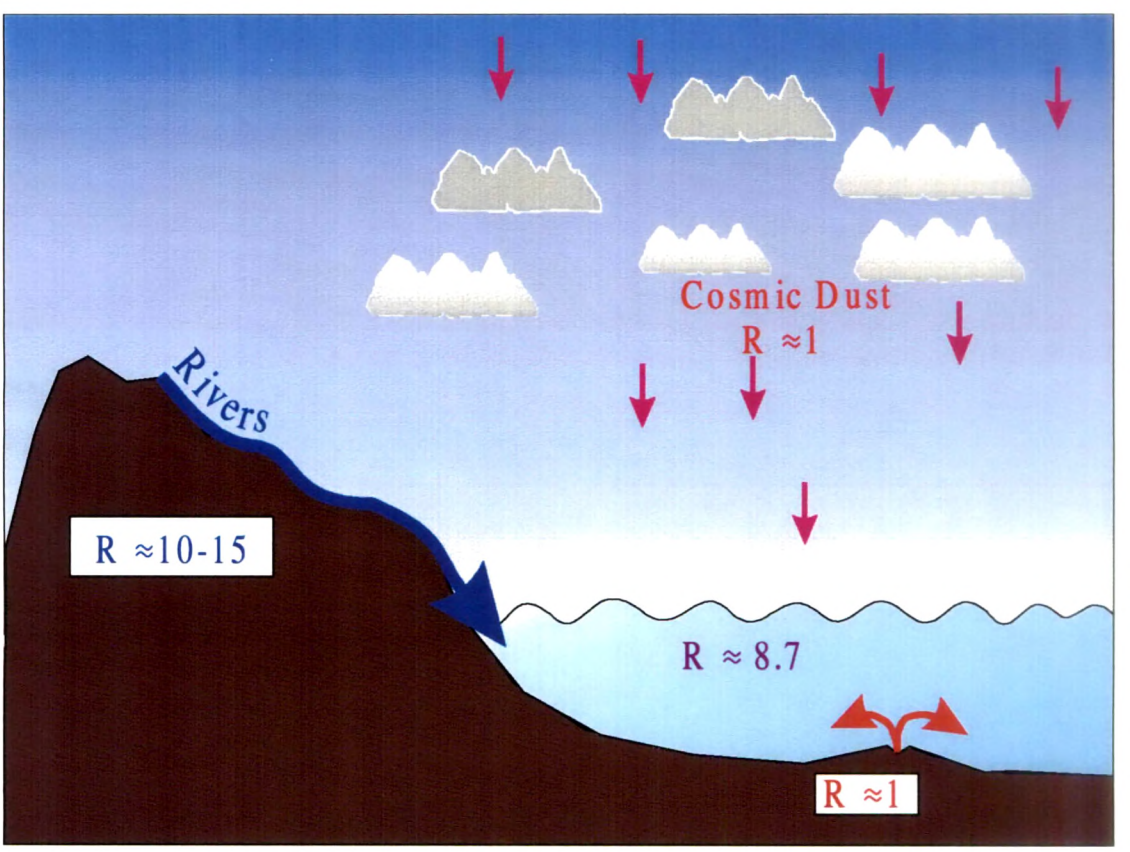

Fig.4.10: Different sources of Os to the ocean. These include the cosmic or extraterrestrial material, hydrothermal input and weathering of submarine basalts and currently eroding continental crust. Among all the sources, the $^{187}Os/^{186}Os$ (R) in the crust is most radiogenic and has values of 10-15. The present day seawater $^{187}Os/^{186}Os$ is ~8.7

to corroborate the suggestion, though there is some debate about the magnitude and sources of the contributions from the Himalaya to the $^{87}Sr/^{86}Sr$ in ocean. Following the Sr analogy, and based on the timing and trend of $^{187}Os/^{186}Os$ evolution in ocean, it was suggested (Pegram *et al.*, 1992; Ehrenbrink *et al.*, 1997; Turekian and Pegram, 1997) that the increase in the $^{187}Os/^{186}Os$ since last ~50 Ma has resulted from intense continental weathering, particularly organic-rich ancient sediments of the Himalaya. Black shales generally contain high concentrations of both Re and Os with Re/Os ratios 10-20 times higher than average crustal materials (Ravizza and Turekian, 1989). As a result the $^{187}Os/^{186}Os$ in old black shales become much higher than that in crustal silicates and their weathering can be significant source of Os isotopes to the sea. This coupled with intense weathering in the Himalaya make the black shales of the region a potential source of radiogenic Os to the ocean. More detailed analysis of Os isotope evolution (Ravizza, 1993; Ehrenbrink *et al.*, 1995; Turekian and Pegram 1997) seem to indicate that, though, both $^{187}Os/^{186}Os$ and $^{87}Sr/^{86}Sr$ show steady increase during the past ~50 Ma, their evolutionary trend seem to be decoupled at different time segments, indicating that a common source for their oceanic increase during the past ~50 Ma, as was initially proposed may not be fully valid. For example, between 25 and 16 Ma $^{87}Sr/^{86}Sr$ rises rapidly towards more radiogenic values whereas the Os isotopic composition remains essentially invariant. This lead Reusch *et al.* (1998) to suggest that weathering of New Guinea Arc and Australian continental margin could also be important in influencing the evolution of these isotope ratios in the ocean.

Detailed discussion and review on the various source (s) contributing to the Os isotope evolution of the ocean, though is beyond the scope of this thesis work, another possible source which can influence the difference in the Os and Sr isotope evolution of seawater is the intense weathering of Gangdese Batholith during the period of 25 to 16 Ma. The study of Indus fan in the northern Arabian Sea indicates that weathering in the western Himalaya was enhanced at ~25 Ma (Whitting and Karner, 1991). In the Southern Tibet, the Kailash conglomerate records the unroofing of the Gangdese batholith of (Copeland, 1997). The time of this deposition has been constrained to be Early Miocene (Copeland, 1997 and references therein) indicating rapid unroofing of Gandese batholith during that period. Copeland *et al.*(1987), based on the Ar-Ar study on the Gangdese

batholith infer that ~ 3 km thickness of the batholith eroded during 25-17 Ma. Isotopic data suggest a largely mantle source for the rocks of the Gangdese, with <30% of crustal contamination (Copeland, 1997 and references therein). The weathering of this batholith may contribute to the decoupling of Sr and Os isotope evolution druing 25-16 Ma as its weathering mostly supply mantle like Os ($^{187}Os/^{186}Os \approx 1$) which would buffer the increase in oceanic $^{187}Os/^{186}Os$, whereas the weathering of granites and gneisses from the Higher Himalaya would continue to increase the $^{87}Sr/^{86}Sr$.

The ideal approach to test the importance of weathering in the Himalaya in contributing to the $^{187}Os/^{186}Os$ is through measurements of the concentration of Os and its isotope composition in rivers draining the Himalaya. But till date there are no measurements of Os in Himalayan rivers. In the absence of such data from the Himalayan rivers, an indirect approach to check the hypothesis is through model calculations of Os flux and $^{187}Os/^{186}Os$ required to account for the observed increase in marine $^{187}Os/^{186}Os$ and whether such requirements can be met by weathering of black shales from the region as they are likely to be the major source of the Os to these Himalayan rivers (Singh *et al.*, 1999). This approach relies on the availability of data on the concentration of Os and its isotopic composition in black shales. Based on the Re-Os isotope analysis of black shales made in this study and models available in literature, their role in contributing to the temporal evolution of oceanic $^{187}Os/^{186}Os$ has been assessed in the following section (Singh *et al.*, 1999).

Following the model of Richter *et al.* (1992) for oceanic Sr isotope evolution the balance equation for ^{187}Os and ^{186}Os in seawater can be written as:

$$\frac{d^{187}N}{dt} = \sum_i {}^{187}J_i - {}^{187}J_o \qquad (4.1)$$

$$\frac{d^{186}N}{dt} = \sum_i {}^{186}J_i - {}^{186}J_o \qquad (4.2)$$

where,

$^{186}J_i$, $^{187}J_i$: input fluxes of ^{186}Os, ^{187}Os from source i to ocean

$^{186}J_o$, $^{187}J_o$: output fluxes of ^{186}Os, ^{187}Os from the ocean

^{186}N, ^{187}N : moles of ^{186}Os and ^{187}Os in ocean

The Os isotopic ratio (R_s) of the ocean is

$$R_s = \frac{^{187}N}{^{186}N} \tag{4.3}$$

Substituting $^{187}N=R_s{}^{186}N$ in Eqn. (4.1) yield:

$$R_s \frac{d(^{186}N)}{dt} + {}^{186}N \frac{dR_s}{dt} = \sum_i {}^{187}J_i - {}^{187}J_o \tag{4.4}$$

Subsituting $\frac{d(^{186}N)}{dt}$ from Eqn. (4.2) in Eqn. (4.4) give:

$$^{186}N \frac{dR_s}{dt} = \sum_i {}^{187}J_i - {}^{187}J_o - R_s\left(\sum_i {}^{186}J_i - {}^{186}J_o\right) \tag{4.5}$$

Eqn. (4.5) is simplified using following assumptions:

(i) Os isotopes do not fractionate during their removal from the ocean, (hence, $^{187}J_o=R_s{}^{186}J_o$)

(ii) The Os isotopic composition of different sources to the ocean can be characterised by an average value, R_i, (thus, $^{187}J_i = R_i\ {}^{186}J_i$). The value of R_i vary with time.

(iii) the total number of moles of ^{186}Os in the ocean (^{186}N) is constant with time.

This yield

$$^{186}N \frac{dR_s}{dt} = \sum_i R_i {}^{186}J_i - R_s \sum_i {}^{186}J_i \tag{4.6}$$

Oceans receive Os isotopes principally from (i) rivers (dissolved and leachable) (ii) dissolution of extraterrestrial materials and (iii) hydrothermal sources and submarine weathering of basalts. The $^{187}Os/^{186}Os$ of the ocean is controlled by the relative fluxes of ^{186}Os from these sources and the $^{187}Os/^{186}Os$ of rivers as the $^{187}Os/^{186}Os$ of the extraterrestrial and hydrothermal components can be considered invariant with time at ~1. Therefore, changes in the magnitude of any of these fluxes and/or $^{187}Os/^{186}Os$ of rivers can cause variation in R_s. Splitting the $^{186}J_i$ term in equation (4.6) into the riverine ($^{186}J_r$) and the non-radiogenic cosmic/hydrothermal ($^{186}J_{nr}$) components, with their corresponding $^{187}Os/^{186}Os$, R_r and R_{nr} respectively, Eqn. (4.6) can be rewritten as:

$$^{186}N \frac{dR_s}{dt} + R_s(^{186}J_r + {}^{186}J_{nr}) = {}^{186}J_r R_r + {}^{186}J_{nr} R_{nr} \tag{4.7}$$

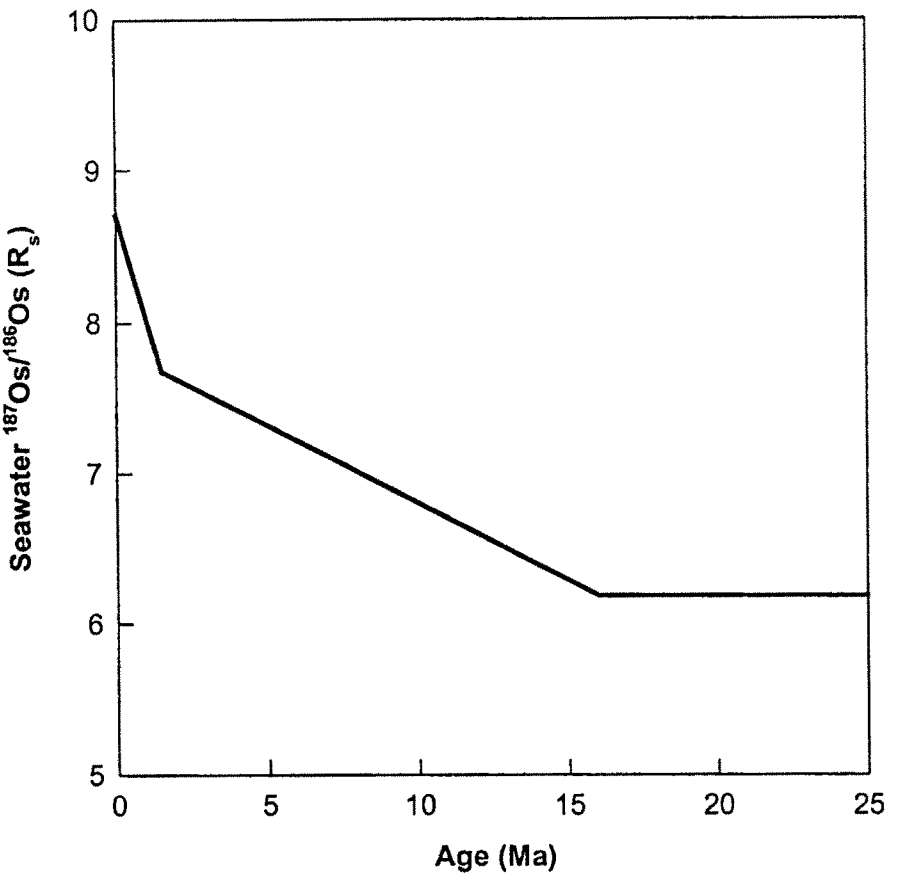

Fig. 4.11: $^{187}Os/^{186}Os$ evolution of sea water during the past 25 Ma. Smooth line is drawn from the data of Ravizza, 1993 . The seawater $^{187}Os/^{186}Os$ evolution can be devided into three segments 25-16 Ma ($R_s \approx 6.2$), 16-1.5 Ma (R_s 6.2 to 7.7) and 1.5 Ma to present (R_s 7 7 to 8.7)

The flux of ^{187}Os from rivers ($^{186}J_rR_r$) would be governed by the intensity of weathering and the $^{187}Os/^{186}Os$ of the drainage basin and any change in either or both of these can effect the riverine ^{187}Os flux and hence the oceanic $^{187}Os/^{186}Os$. Climate and tectonics are important in influencing the intensity of weathering and therefore the flux of Os transported to oceans. The degree of weathering also determines the proportion of Os isotopes contributed to rivers by various lithologies and hence the value of R_r. The $^{187}Os/^{186}Os$ of the basin can also vary because of radioactive ingrowth of ^{187}Os from the decay of ^{187}Re (Ravizza and Ehrinbrink, 1998). This can monotonically increase the $^{187}Os/^{186}Os$ of the basin with time, the rate of change being dependent on its $^{187}Re/^{186}Os$

abundance ratio. Tectonic processes can cause changes in the lithology of the drainage basin which in turn can also contribute to changes in its $^{187}Os/^{186}Os$.

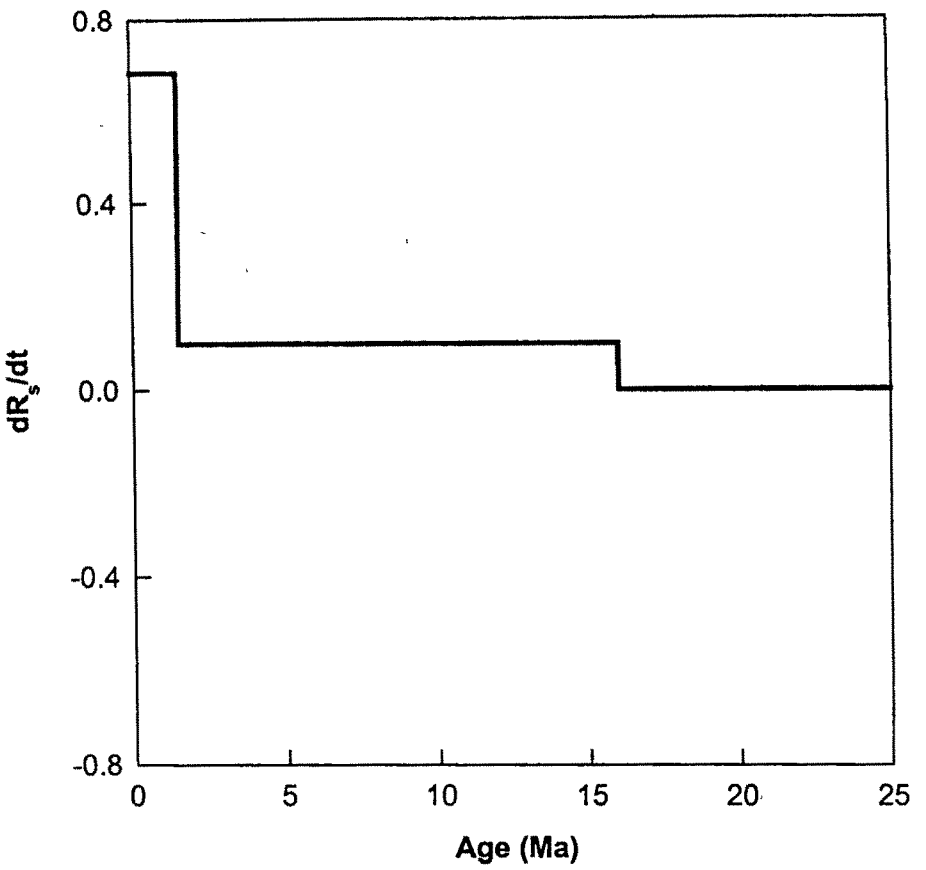

Fig. 4.12 Rate of change of $^{187}Os/^{186}Os$ in ocean. R_s has been increasing at a nearly constant rate of 0.1 Ma^{-1} during the interval 16-1.5 Ma. And much more rapidly during the recent ~1.5 Ma (dR_s/dt 0.68 Ma^{-1}). Prior to 16 Ma it was constant at 6.2.

Available data (Pegram *et al.* 1992; Ravizza, 1993; Turekian and Pegram, 1997; Reusch *et al.* 1998) on the $^{187}Os/^{186}Os$ of oceans show that its evolution during the past 25 Ma can be broadly divided into three segments (Fig. 4.11), it was nearly constant at 6.2 during 25-16 Ma, it increased uniformly from 6.2 to 7.7 between 16 Ma to 1.5 Ma with a slope of 0.10 Ma^{-1} (Fig. 4.12) and far more rapidly during the recent 1.5 Ma at rate of 0.68 Ma^{-1} (Fig. 4.12). The objective of this modelling exercise is to evaluate the changes required in $^{186}J_r$ or R_r to produce the measured temporal variations in R_s. The approach followed is to obtain an estimate of the contemporary $^{186}J_{nr}$ based on material balance considerations and using available data on N, R_s, $^{186}J_r$ and R_r (Table 4.4).

Table 4.4: Present day Os fluxes and isotopic ratios*

$^{186}J_r$	= 15.8 moles y^{-1} (total Os flux ≈1160 moles y^{-1})
R_r	= 11.0
$^{186}J_{nr}$**	= 4.72 moles y^{-1} (total Os flux ≈300 moles y^{-1})
R_{nr}	= 1
^{186}N	= 3.1×10^5 moles (C_s ≈ 16 fmoles kg^{-1})
R_s	= 8.7

* from Sharma and Wasserburg (1997) and Sharma *et al.*, (1997)

** calculated from material balance considerations to produce present day R_s = 8.7.

Assuming that $^{186}J_{nr}$ has remained the same at the present day value during the past 25 Ma, the changes required either in $^{186}J_r$ or R_r are calculated to account for the observed variations in R_s (Fig. 4.11). There is very little data on the Os concentration and $^{187}Os/^{186}Os$ of rivers. So far only results for four rivers are available in literature (Sharma and Wasserburg, 1997). The calculations that follow, assumes that the mean Os concentration and the $^{187}Os/^{186}Os$ of these four rivers is representative of the present day global river (Table 4.4). The $^{187}Os/^{186}Os$ of these rivers range between 8.8-14.4 (mean 11.0) and Os concentrations 2.6-8.6 pg kg^{-1} (mean 5.9 pg kg^{-1}). The mean $^{187}Os/^{186}Os$ of 11.0 is quite similar to the value of 10.5 ± 0.5 reported by Esser and Turekian (1993) for $^{187}Os/^{186}Os$ of erodable continental crust. The calculation has been done both for the global rivers and the Himalayan rivers.

Case I. Temporal variations in R_s is only due to change in J_r (R_r is kept constant).

Using equation (4.7) and the available values for different parameters, $^{186}J_r$ for the global rivers has been calculated with time. Figure 4.13 presents the changes in $^{186}J_r$ with time required to produce the measured $^{187}Os/^{186}Os$ variations in seawater keeping R_r constant at 11.0. The model shows that the global riverine flux of ^{186}Os, $^{186}J_r$, has to increase from 5.1 moles y^{-1} 16 Ma ago to 9.5 moles y^{-1} 1.5 Ma ago and more rapidly to

the present day value of 15.8 moles y^{-1}. (for R_r = 11.0, this would translate to total Os flux of ~370 moles y^{-1} at 16 Ma and 1160 moles y^{-1} today). If enhanced weathering of black shales from the Himalaya accounts for this increase in $^{186}J_r$, as has been suggested (Pegram *et al.* 1992) the required variation in $^{186}J_{HTP}$ with time would be as given in Fig. 4.14. This calculation has been made by splitting the river flux term in Eqn. 4.7 into two

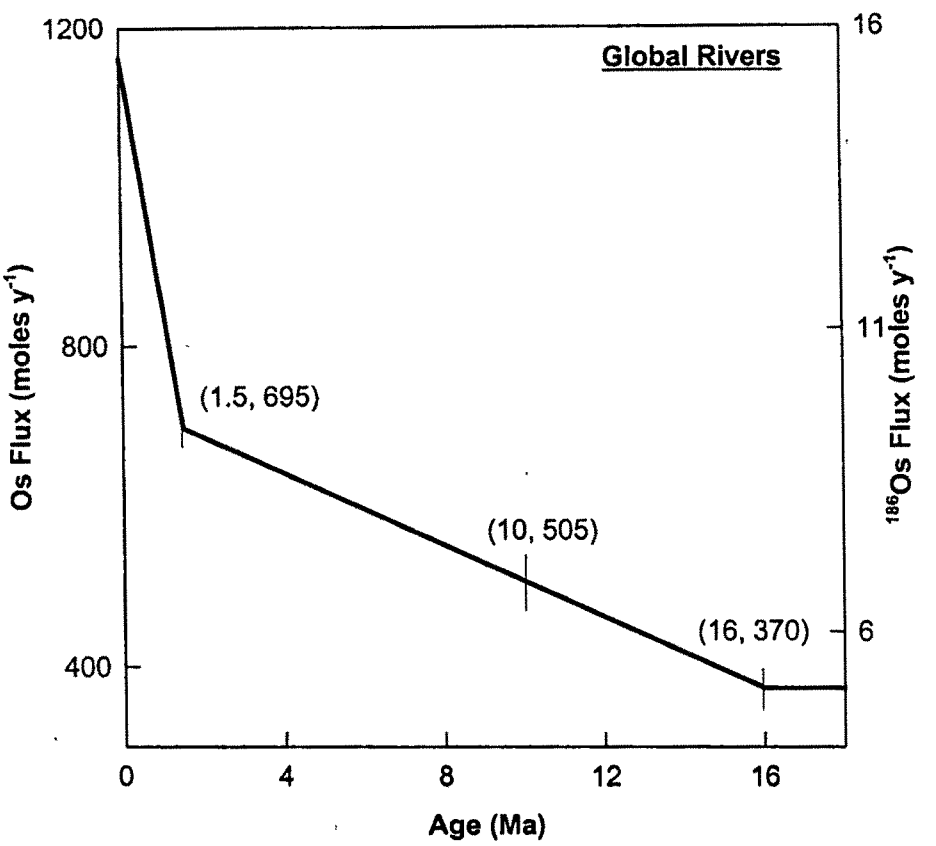

Fig. 4.13: Temporal variations in total Os and ^{186}Os flux required from global rivers to reproduce the observed Os isotopic composition of seawater. The total Os flux required at 16, 10 and 1.5 Ma are given in parenthesis.

components, one representing the flux from HTP rivers (J_{HTP}) and the second from all the other rivers, J_{rest}, (i.e. excluding those draining the HTP).

$$^{186}N\frac{dR_s}{dt}+R_s\,(^{186}J_{rest}+{}^{186}J_{HTP}+{}^{186}J_{nr}) = (^{186}J_{HTP}R_{HTP}+{}^{186}J_{rest}R_{rest})+{}^{186}J_{nr}R_{nr} \quad (4.8)$$

$^{186}J_{rest}$ and $^{186}J_{HTP}$ 16 Ma ago are taken to be 4.6 and 0.51 moles y^{-1} respectively in proportion to their water discharge (HTP rivers make up ~10% of global river discharge. Taking Os flux via rivers in proportion to water discharge, $^{186}J_{rest}$ would be 4.6 moles y^{-1}, 90% of the Os flux of 5.1 moles y^{-1}16 Ma ago,). The results (Fig. 4.14) show that $^{186}J_{HTP}$

has to increase from 0.51 to 4.9 moles y^{-1} during 16 to 1.5 Ma and far more rapidly to 11.3 moles y^{-1} today. The calculated present day $^{186}J_{HTP}$ value of 11.3 moles y^{-1} (≈ 830 moles y^{-1} total Os flux) would correspond to an Os concentration of ~40 pg ℓ^{-1} in these rivers. The average Os concentration in black shales from the Maldeota and Durmala mines is ~2 ng g^{-1}. If this value is typical of Os concentration in black shales of the Himalaya, then to yield ~40 pg Os $\ell^{-1}$of river water, it requires that Os from ~20 mg of

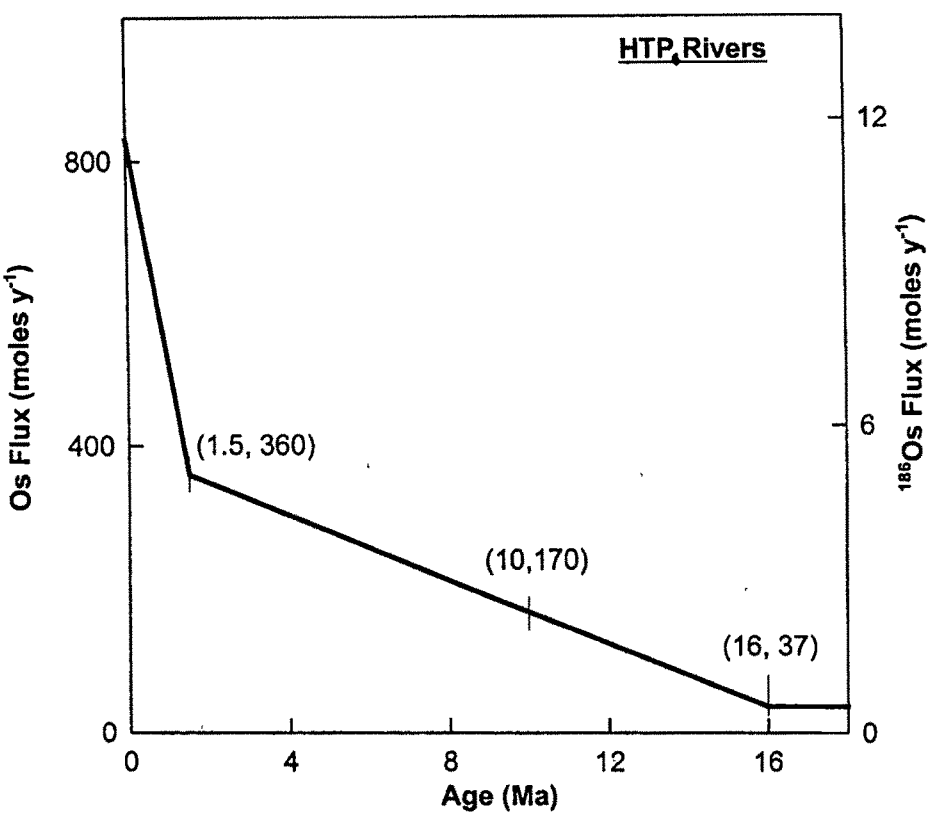

Fig. 4.14: Osmium flux required from HTP rivers if all the observed changes in oceanic $^{187}Os/^{186}Os$ results from Os supply from the Himalayan-Tibetan-Plateau rivers. Calculation made by assuming that the $^{187}Os/^{186}Os$ of the global (R_{rest}) and the Himalayan rivers (R_{HTP}) has remained constant at 11.0.

black shales has to be released per liter of river water. (if the highest concentration of 13.5 ng g^{-1} measured in KU92-56, Table 4.2, is excluded from averaging, the mean Os in the mine samples would be ~1 ng g^{-1} and Os from ~40 mg of black shale would have to be released per liter of river water). There is no data on the Os concentration of Himalayan rivers, however, there are some measurements of Re in the Ganges and the

Brahmaputra (Colodner *et al.* 1993). The Re concentration in these rivers at their mouth is 1-2 ng ℓ^{-1}. If all this Re is derived from black shales, with a concentration of ~60 ng g^{-1} (mean of Maldeota and Durmala black shales) it would suggest that Re from ~15-30 mg of black shale is released per liter of river water, quite similar to that required to maintain the Os concentration of ~40 pg ℓ^{-1}. This seems to indicate that it may be possible for the rivers draining the Himalaya to acquire Os concentration of ~40 pg ℓ^{-1} through weathering of black shales and thus account for the temporal variations in R_s.

Case II: Changes in $^{187}Os/^{186}Os$ in seawater is only due to changes in R_r ($^{186}J_r$ is constant).

These calculations (Eqn. 4.8), made by keeping $^{186}J_r$ constant over 16 Ma at today's value of 15.8 moles y^{-1} (Table 4.4), show that R_r has to increase from 7.7 at 16 Ma to 9.7 at 1.5 Ma and to 11.0 at present (Fig. 4.15) to reproduce the observed variations in R_s. If this entire increase has to result from HTP rivers, the corresponding change in their $^{187}Os/^{186}Os$ with time has to be from 7.7 at 16 Ma ago to 27.1 at 1.5 Ma and 40.5 today (Fig. 4.16). In this calculation, $^{186}J_{rest}$ is kept at today's value of 14.2 moles y^{-1} (in proportion to water discharge; 90% of today's ^{186}Os flux, 15.8 moles y^{-1}, Table 4.4) and R_{rest} at 7.7, the ratio 16 Ma ago. The present day requirement of $R_{HTP} \approx 40.5$, though is within the range measured in this study for black shales from the underground mines, it is on the higher side of the mean ratio ~23 measured in them (only three out of 30 black shales analysed in this study had $^{187}Os/^{186}Os$ in excess of 40.5) and those reported for leachable fraction of Ganga sediments 16.93 and 15.37 from Varanasi and Patna respectively (Pegram *et al.*, 1994).

Recently, Ravizza and Ehrenbrink (1998) have suggested an interesting possibility to bring about changes in R_s. Their model argues that bulk of the Os to the ocean is supplied via the weathering of organic rich sediments typically having $^{187}Re/^{186}Os$ of ~6000. This high $^{187}Re/^{186}Os$ would monotonically increase the $^{187}Os/^{186}Os$ of the sediments due to radioactive decay of ^{187}Re, at a rate of 0.1 Ma^{-1}. If the $^{187}Os/^{186}Os$ of rivers draining these sediments also increase at the same rate, then it would account for a significant fraction of that required to produce the observed temporal variations in R_s during 16-1.5 Ma. If, however, the $^{187}Re/^{186}Os$ of the sediments being weathered are

~1000-2000, similar to those measured in this study in black shales from the Lesser Himalaya, then the radiogenic ingrowth would be only a minor component contributing to the required increase in R_r (Fig. 4.15).

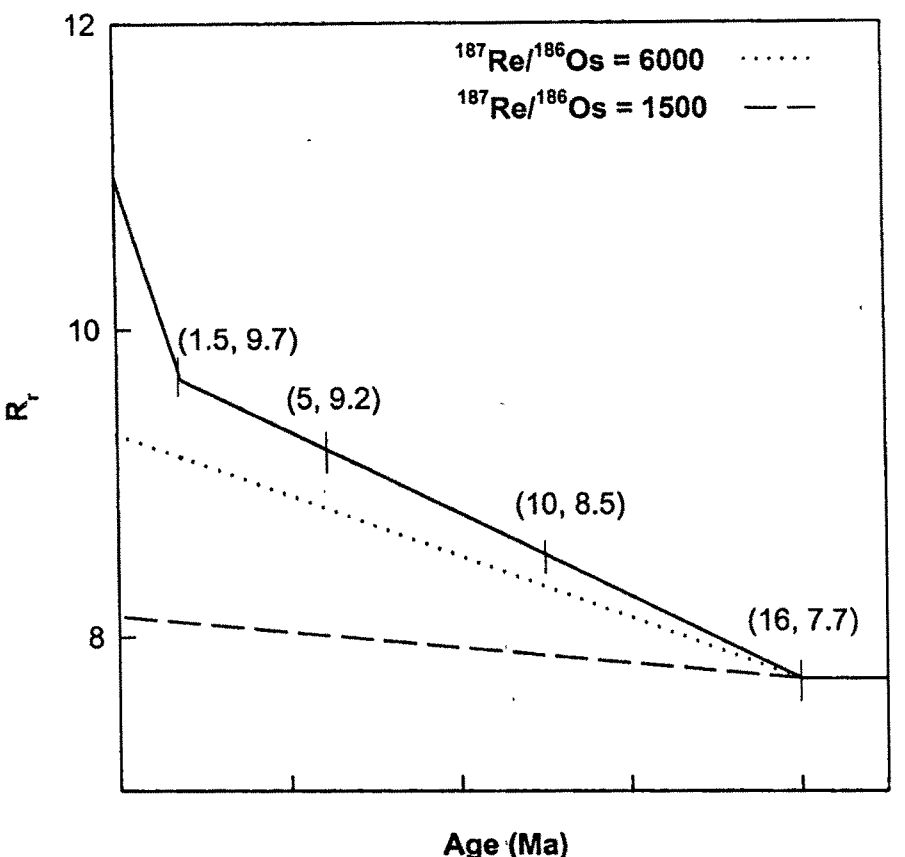

Fig. 4.15: Changes required in riverine (global) $^{187}Os/^{186}Os$ to reproduce the observed changes in seawater $^{187}Os/^{186}Os$ during the past ~16 Ma. The calculation assumes that change in seawater $^{187}Os/^{186}Os$ is only due to changes in riverine Os ratio. The numbers given in the parenthesis corresponds to values of R_r at 16, 10, 1.5 Ma ago. The two dashed lines correspond to growth of $^{187}Os/^{186}Os$ in the drainage basin over 16 Ma, for $^{187}Re/^{186}Os$ = 6000 (typical of organic rich sediments; Ravizza and Ehrenbrink, 1998) and $^{187}Re/^{186}Os$ = 1500 (typical of black shales measured in this study from the Lesser Himalaya).

In addition to the above calculations, it is possible to estimate the Os flux required from HTP rivers to yield present day value of R_s by changing both $^{186}J_{HTP}$ and R_{HTP}. We use the mean of the reported (Pegram *et al.*, 1994) $^{187}Os/^{186}Os$ in leachable component of the Ganga river sediments at Varanasi and Patna, 16.2, as representative of the HTP rivers at present, instead of 11.0 used in earlier calculations (case I). (the other values are $^{186}J_{rest}$ = 4.6 moles y^{-1} and R_{rest} = 11.0). This yields a value for the present day $^{186}J_{HTP}$

~3.4 moles y^{-1}, corresponding to an Os concentration of ~14 pg ℓ^{-1} in HTP rivers. This concentration can be more easily accommodated by weathering of black shales and also is well within the range of 3-25 pg kg^{-1} for Os in rivers reported by Sharma and Wasserburg (1997) and Levasseur *et al.* (1998). The parametric values used in the calculation would make R_r ~13, higher than the mean of the four river water values (Table 4.4); but within their range, 8.8-14.4 (Sharma and Wasserburg, 1997).

The rapid increase in R_s during the recent 1-2 Ma (Fig. 4.14), is difficult to be explained, eventhough the changes required in R_r and J_r to account for this have been calculated above. It is interesting to note that the sediment accumulation rate in the

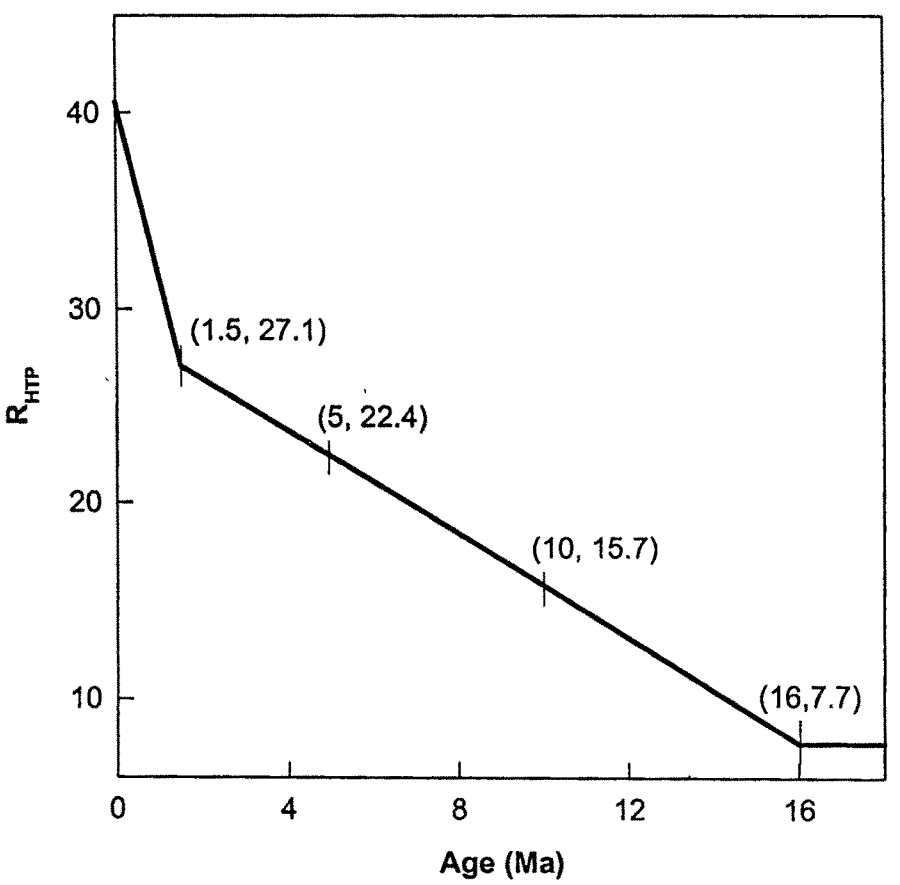

Fig. 4.16: Required variations in $^{187}Os/^{186}Os$ of HTP rivers if they account for the entire increase in seawater $^{187}Os/^{186}Os$ during the past ~16 Ma. This calculation assumes $^{186}J_{rest}$ = 14.2 moles y^{-1} and R_{rest} = 7.7, the values 16 Ma ago to be constant. The R_{HTP} values at 16, 10, 5and 1.5 Ma are given in parenthesis.

Bengal Fan was about four times higher during the past ~1 Ma compared to that during 1-15 Ma (Cochran, 1990; Gartner, 1990). This enhanced sediment accumulation has been been attributed to intense weathering during Pliocene-Pleistocene glaciations and the direct dumping of river suspended material to continental slope due to lowering of sea level (Cochran, 1990). Studies on the fate of Os isotopes associated with river particles when they come in contact with seawater are too few to make any generalisation. Reisberg *et al.* (1997) based on studies of leachable and bulk Os in sediments from the Bengal Fan concluded that leachable Os from river suspended matter is released to seawater prior to their deposition on the seafloor and that it is an important source of Os to the oceans. They calculated that ~23 % of the seawater increase can be accounted for by the release of Os from the sediments in the Bengal Fan. More recently, Porcelli *et al.* (1998) based on the distribution of dissolved Os in the Columbia river estuary reported that it exhibits an overall conservative behaviour, though signatures of its addition/removal are also evident in its distribution. The intense glacial weathering and large supply of river suspended matter directly to the slope regions may have a role to play in the rapid increase in R_s during the past ~1 Ma. Thus the enhanced amount of sediment supply from the Himalaya can provide higher leachable Os to the seawater and this leachable Os coupled with the dissolved phase can give rise to the present observed seawater Os isotope curve, however, it is difficult to quantify their significance at present.

It is important to mention here that all the above model calculations are based on the assumption that the Os flux to the oceans derived from cosmic/mantle materials have remained constant at today's value over the past ~25 Ma. The results of the calculations critically depend on the validity of this assumption.